JOURNAL OF OPTOELECTRONICS AND ADVANCED MATERIALS Vol. 10, No. 4, April 2008, p. 780 - 782

XPS study of RNi_4B compounds, where R = Nd, Tb, Dy, Ho and Er

C. LAZĂR, E. BURZO, M. NEUMANN[a,*]
Faculty of Physics, Babes-Bolyai University Cluj-Napoca, Romania
[a]*Fachbereich Physik, Universität Osnabrück, Germany*

The RNi_4B compounds with R = Nd, Tb, Dy, Ho and Er crystallize in $CeCo_4B$-type structure. XPS measurements were performed at room temperature. The Ni $2p_{1/2}$ and Ni $2p_{3/2}$ core level lines reproduce well those of pure nickel. In all samples, the presence of Ni 6 eV satellite line was shown. This indicates the presence of holes in Ni 3d band, in agreement with magnetic measurements. The R 4d core levels are similar to those evidenced in pure R metals. The 4f orbitals keep their localized character and therefore the XPS spectra show multiplet structures. The small energy shift of R4d and R4f core level lines, as compared to R metals, may be correlated with minor changes in shielding which result from modification of electron concentrations when compounds are formed.

(Received February 25, 2008; accepted April 2, 2008)

Keywords: Rare earth compounds, XPS studies

1. Introduction

The RNi_4B compounds, where R is a rare earth, crystallize in a $CeCo_4B$ type structure, having P6/*mmm* space group [1, 2]-Fig.1. The rare earth atoms occupy two nonequivalent positions: 1a and 1b, the Ni atoms are situated in 2c and 6i positions and the B atoms in 2d position. The magnetic properties of these systems were analysed [3-5]. The XPS measurements on RNi_4B with R = Ce, Pr and Nd [6] showed the presence of hybridization effects. The magnetic moments at 0 K was shown to be very weak and dependent on the rare-earth partner. In the paramagnetic range an effective magnetic moment of 1.8 μ_B/Ni atom was shown [5].

As an on going work on the matter we report in this paper the results of XPS measurements on RNi_4B compounds with Tb,Dy,Ho, Er and Nd.

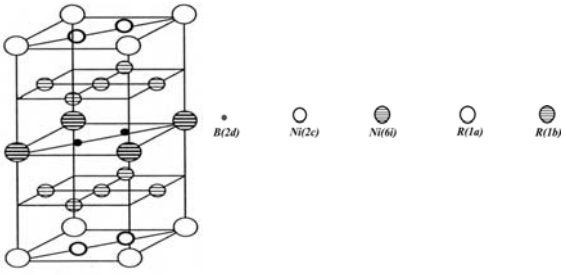

Fig. 1. The $CeCo_4B$-type structure.

2. Experimental

The RNi_4B compounds were prepared by arc-melting the high purity elements, under argon atmosphere. The samples were remelted several times to ensure good homogeneity and then were thermally treated at 850 ^oC. The X-Ray analyses show the presence of a single phase. The compunds cristallize in a $CeCo_4B$ – type structure.

XPS measurements were performed using a PHI 5600 MultiTechnique System. All spectra were recorded at room temperature, using monochromatized Al K_α radiation (1486.6 eV). The total resolution, as determined at the Fermi level of a gold foil, was about 0.3-0.4 eV. The binding energies are given with reference to the Fermi level. The $4f_{7/2}$ gold level was found at 84.0 eV binding energy. All spectra were recorded in vacuum below $5x10^{-10}$ mbar.

Band structure calculations were performed using the LMTO-ASA method [7,8].

3. Experimental results

Band structure calculations were performed for compounds with Gd, Tb, Dy, Ho and Er. The total densities of states are represented in Fig.2, for compounds with R = Gd, Dy, Er. The Ni atoms have a very small magnetic moment, M_{Ni}, at 0 K. The M_{Ni} values increase linearly with the De Gennes factor from 0.02 μ_B (R = Er) to 0.08 μ_B (R = Gd) for 2c sites and from 0.01 μ_B (Er) to 0.04 μ_B (Gd) for 6i sites. These moments are antiparallely oriented to those of rare-earths.

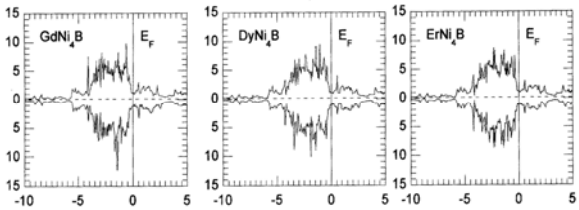

Fig. 2. Total densities of states, for RNi_4B (R=Gd,Dy,Er).

The Ni(2c) magnetic contributions determined from band structure calculations are higher than those of Ni(6i),

because of different local environments. The effective Ni moments are nearly constant and close to 1.8 μ_B/atom.

The Ni $2p_{1/2}$ and Ni $2p_{3/2}$ core level lines are plotted in Fig. 3. The values of the binding energies in RNi_4B compounds and pure Ni are listed in Table 1. The line positions are not modified in compounds as compared to pure Ni.

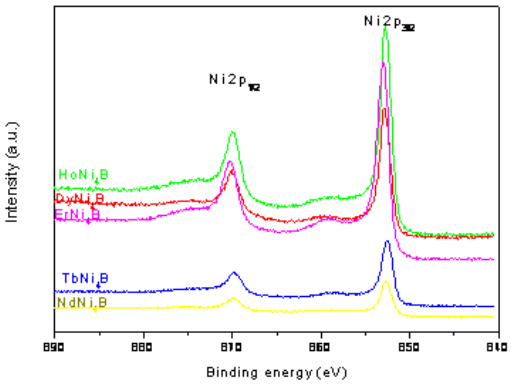

Fig. 3. Ni $2p_{1/2}$ and Ni $2p_{3/2}$ core levels.

Table1 .*The binding energies of Ni 2p in Ni and RNi_4B compounds.*

Compound	Ni $2p_{3/2}$	Ni $2p_{1/2}$
Ni	852.7 ± 0.1	869.97 ± 0.1
$NdNi_4B$	852.306 ± 0.1	869.4 ± 0.1
$TbNi_4B$	852.17± 0.1	869.37± 0.1
$DyNi_4B$	852.85± 0.1	870.1± 0.1
$HoNi_4B$	852.59± 0.1	869.83± 0.1
$ErNi_4B$	853.02 ± 0.1	870.48 ± 0.1

The Ni 6 eV sattelite line appears in the RNi_4B compounds, with R = Tb, Dy, Ho, Er, at the same binding energy as in pure Ni (858 ± 0.1 eV). The line intensity is lower than in case of pure Ni, suggesting that the number of holes is diminished as compared to Ni 3d band. This is in agreement with the smaller effective Ni moment determined in the paramagnetic range (1.8 μ_B/atom as compared to μ_{ef} (Ni^{2+}) = 2.83 μ_B/atom) [9]. In the case of $NdNi_4B$ compound, the Ni 6 eV line intensity cannot be no ambiguously analysed, due to the superposition with the 4d lines of the rare earth.

The rare earth 4d core level spectra of the rare earths are given in Fig. 4. The small shifts that appear in RNi_4B compounds compared to pure metals were attributed to minor changes in shielding which result from modification of electron concentration [10].

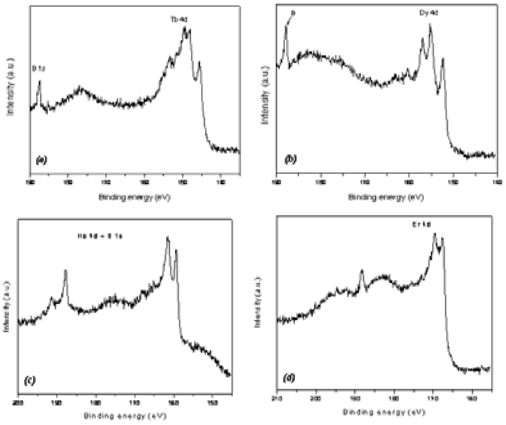

Fig. 4. Core level lines of of RNi_4B compounds with R = Tb (a), Dy (b), Ho(c) and Er(d).

The Nd 3d core level lines and 4d ones of R = Dy, Ho, Tb, Er were decomposed in the main and sattelite lines as in pure metals [11], and are given in Table 2. The binding energies show only small shifts as compared to the values determined in pure metals, indicating a similar electronic configuration. In the case of $NdNi_4B$ compound, the $3d_{3/2}$ and $3d_{5/2}$ lines of Nd were identified at 1004.45 eV and 980.68 eV binding energy, respectively, little shifted as compared to pure Nd. This may correspond to a contamination with Nd_2O_3 of the sample surface. Also, the spin-orbit splitting of the 3d lines is higher than in case of pure metal (23.77 eV vs 22.6 eV).

Table 2. Binding energie (BE)s of rare earths in pure elements and in RNi_4B compounds.

Element	RE lines	BE in pure element (eV)	BE in compound (eV)
Nd	$3d_{3/2}$ $3d_{5/2}$	1003 980,8	1004.45± 0.2 980.68± 0.2
Tb	4d	145.95 147.98 150.55 153.91	145.49± 0.2 148.61± 0.2 149.73± 0.2 153.05± 0.2
Dy	4d	152.4 153.31 155.12 156.91	152.3 ± 0.2 153.6 ± 0.2 154.99 ± 0.2 156.95 ± 0.2
Ho	4d	159.59 161.83	159.37± 0.2 161.41± 0.2
Er	4d	167,3 169.3	167.67± 0.2 169.63± 0.2

The valence bands spectra of RNi_4B compounds with R = Tb(a), Ho(b), Er(c) and Nd(d) are given in Fig. 5.

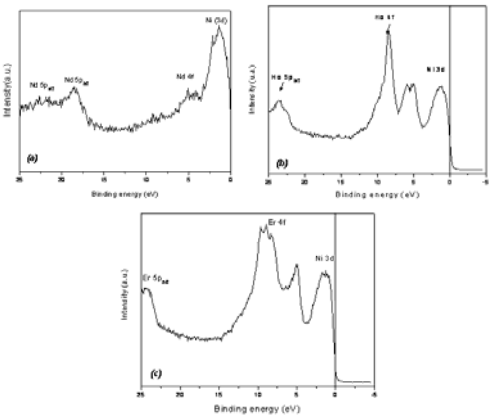

Fig. 5. Valence bands spectra of RNi4B compounds with R = Nd(a),Ho(b),Er(c).

The densities of states at the Fermi level are mainly determined by the Ni 3d ones. These values decrease as compared to those of pure Ni, due to the Ni3d-R5d and Ni3d-B2p hybridizations effects. The low density of states at the Fermi level may be correlated with the band structure calculations, that also evidence a lower density of states at the Fermi level.

The XPS valence band spectra show multiplet structures, indicating the presence localized character of the 4f orbitals. This is a common feature of all studied RNi_4B compounds. The small shifts in the 4f line positions as for 4d core lines may be correlated with changes in shielding, which result from the modification of electron concentrations. The XPS valence band spectra of $NdNi_4B$ cannot be unambiguously analysed, because of the superposition of the Nd 4f and Ni 3d lines. Qualitatively can be concluded only that there is a decrease of state densities at the Fermi level due to hybridization effects, as already mentioned.

4. Discussions

In RNi_4B compounds, nickel atoms have a very small magnetic moments at 0 K. At temperatures higher than the Curie points, effective nickel moments were determined. In addition, the XPS measurements, performed at room temperature ($T > T_c$), evidenced the presence of holes in Ni3d band. The above behaviour can be analysed in models which take into account the electron correlations effects in d-band as spin fluctuation model [12] or dynamical field theory [13]. These models reconcile the dual character of electron which as particle requires a real space description and as a wave, a momentum space description.

The spin fluctuation model considers the balance between the frequencies of longitudinal spin fluctuations which are determined by their lifetime and of transverse fluctuations which are of thermal origin. These effects lead to the concept of temperature induced moment. The moments are localized in q space. The effective nickel moments are smaller than that of Ni^{2+} considering only spin contribution (2.83 μ_B). This is the result of hybridization of Ni3 band with B2p and R5d ones which determines the diminution of nickel moments in agreement with the intensity decrease of 6 eV satellite line.

The magnetic behaviour of nickel in the present system may be also analysed in dynamical mean field theory, DMFT [13] combined with the standard LDA band calculations (LDA + DMFT) [14]. In a strongly correlated system, leading Curie-Weiss behaviour, at high temperatures is predicted. For an itinerant electron system, the time dependence of the correlation function results in a temperature dependence of mean square amplitude of local spin. Fluctuating moments and atomic like configurations are large at short time. The moments are reduced at larger time scale, corresponding to a more band like less correlated electronic structure at the Fermi level.

Acknowledgement

The work was acheved under contract COSTEMSEC Nr. 2-CEEX-06-11-98/2006.

References

[1] Y. B. Kuz'ma, M. P. Khaburskaya, Izv. Akad. Nauk SSSR, Neorg. Mater. **11**, 1893 (1975).
[2] F. E. Spada, H. Oesterreicher, R. C. Bowman Jr., M. P. Guse, Phys. Rev. B. **30**, 9 (1984).
[3] N. M. Hong, T. Holubar, G. Hilscher, M. Vybornov, P. Rogl, IEEE Trans. – Magn. **30**, 4966 (1994).
[4] T. Tolinski, A. Kowalczyk, A. Szlaferek, M. Timko, J. Kovac, Solid State Commun. **122**, 363 (2002); T. Tolinski, A. Kowalczyk, A. Szlaferek, B. Ardrzejewski, J. Kovac, J. Timko, J. Alloys Comp. **347**, 31 (2002); T. Tolinski, Pugaczawa-Michalska, G. Chelkowska, A. Szlaferek, A. Kowalczyk, Phys. Stat Solidi (b) **231**, 446 (2002).
[5] P. Vlaic, N. Bucur, C. Lazăr, E. Burzo, J. Optoelectron. Adv. Mater. **8**, 490 (2006).
[6] T. Tolinski, A. Kowalczyk, G. Chelkowska, Phys. Letters **A308**, 75 (2003).
[7] O. K. Andersen, Phys. Rev. B. **12**, 3061 (1975).
[8] O. K. Andersen, O. Jepsen. D. Glötzel, in Highlights of Condensed Matter Theory, ed. F. Bassani, F. Fumi, M. P. Tosi, New Holland, 1985.
[9] C. Lazăr, E. Burzo, AIP Conf. Proceedings **899**, 782 (2007).
[10] E. Burzo, S. G. Chiuzbăian, M. Neumann, M. Văleanu, L. Chioncel, I. Creangă, J. Appl. Phys. 92 12, 7362 (2002), E. Burzo, J. Optoelectron. Adv. Mater. **9**, 1113 (2007).
[11] B. Vincent Crist, Handbook of Monochromatic XPS Spectra, vol. I, XPS International Inc., 1999.
[12] T. Moiya, J. Magn. Magn. Mat. **100**, 201 (1991).
[13] A. Georges, G. Kothar, W. Krauth, M. J. Rosenberg, Rev. Mod. Phys. **68**, 13 (1996).
[14] A. I. Lichtenstein, H. Katsnelson, G. Kotliar, Phys. Rev. Lett. **87**, 067205 (2001).

*Corresponding author: Manfred.Neumann@uos.de